Analytical Methods

Discrimination of structurally similar odorous molecules with various concentrations by a nanomechanical sensor

Journal:	*Analytical Methods*
Manuscript ID	AY-COM-05-2018-001224.R1
Article Type:	Communication
Date Submitted by the Author:	13-Jun-2018
Complete List of Authors:	Minami, Kosuke; National Institute for Materials Science, International Research Center for Materials Nanoarchitectonics (MANA) Shiba, Kota; National Institute for Materials Science (NIMS), International Center for Materials Nanoarchitectonics (MANA) Yoshikawa, Genki; National Institute for Materials Science International Center for Materials Nanoarchitectonics

Journal Name

COMMUNICATION

Discrimination of structurally similar odorous molecules with various concentrations by a nanomechanical sensor

Received 00th January 20xx,
Accepted 00th January 20xx

DOI: 10.1039/x0xx00000x

www.rsc.org/

Kosuke Minami,*[a,b] Kota Shiba[a,b] and Genki Yoshikawa*[a,b,c]

A pattern recognition-based chemical sensor array is an efficient approach to discriminating odours, while the fluctuation in concentration of odorous molecules often results in concentration-dependent patterns rather than ones based on chemical properties. Here we present the discrimination of odorous molecules based on the chemical properties with the reduced influence of their concentrations in a wide range from ppm to ppb levels using a nanomechanical sensor. Extraction of effective features, which are less affected by concentrations of odorous molecules, from sensing signals leads to successful discrimination of each chemical species even in a series with similar physical structures.

Odours have direct effects on human behaviour and can affect our quality of life, for examples, recognition of an environmental problem, food safety and health conditions. Various gas measurement systems have been widely investigated to detect and identify diverse odours for decades.[1] Recently, chemical sensor arrays have been developed and a wide range of applications have been demonstrated.[2–5]

A chemical sensor array directly measures odours as a pattern without separation of each odorous molecule in contrast to a chromatographic approach. Since the pattern is extracted from sensing signals, it is usually perturbed by the fluctuation in concentration of odorous molecules. Moreover, it is rather difficult to discriminate structurally similar odorous molecules using chemical sensors because such molecules tend to induce similar signals owing to the similar physicochemical interaction with sensing materials. Although the conventional chromatographic approaches, *i.e.* gas chromatography/mass spectrometry (GC-MS), can identify and quantify most odorous molecules even with slight structural differences, such approaches require bulky instrumentation. Thus, a compact chemical sensor array is capable of discriminating structurally similar odorous molecules without being perturbed by the fluctuation in concentrations has been highly demanded. While some studies reported the discrimination of structurally similar odorous molecules by a chemical sensor array with pattern recognition,[6,7] it is still challenging to identify such molecules with various concentrations.

In this study, we demonstrate robust discrimination of structurally similar odorous molecules in a wide range of concentrations. Among various kinds of chemical sensor arrays, we focus on a nanomechanical sensor, especially a Membrane-type Surface stress Sensor (MSS), which can be operated by a compact system and exhibits high sensitivity to various odorous molecules depending on the receptor materials.[8–10] In the case of so-called static mode operation of nanomechanical sensors including MSS, sensing signals are given by mechanical stress/strain induced by the dynamic responses of a receptor layer to adsorption/desorption of molecules. Accordingly, in principle, odorous molecules having structural similarity are apt to induce similar sensing signals because of their similar molecular volume.[8,11] Thus, as model target systems for the chemical discrimination of odorous molecules with the minimal physical effect, we have investigated two series of structurally similar molecules (cluster numbers of 7 and 11, Fig. 1) with various concentrations ranging from 3500 ppm to 97 ppb.[12] Through the investigation of sensing signals in both adsorption and desorption steps, the features having less effect of variation in concentration have been extracted. Based on the chemical fingerprints composed of such effective features, structurally similar odorous molecules have been successfully discriminated even with the variation in concentration.

To investigate the capability in identification of the odorous molecules with the structural similarity, it is important to prepare a highly sensitive receptor layer of MSS. According to our previous study,[13] a response of a nanomechanical sensor is strongly affected by the physical properties of a receptor layer, such as Young's modulus and thickness. Among diverse

[a] Center for Functional Sensor & Actuator (CFSN), National Institute for Materials Science (NIMS), 1-1 Namiki, Tsukuba 305-0044, Japan. E-mail: MINAMI.Kosuke@nims.go.jp (K. M.) and YOSHIKAWA.Genki@nims.go.jp (G. Y.)
[b] International Center for Materials Nanoarchitectonics (MANA), National Institute for Materials Science (NIMS), 1-1 Namiki, Tsukuba 305-0044, Japan.
[c] Materials Science and Engineering, Graduate School of Pure and Applied Science, University of Tsukuba, 1-1-1 Tennodai, Tsukuba, Ibaraki 305-8571, Japan.
† Electronic Supplementary Information (ESI) available: Detailed experimental section, additional signal responses, and additional PCA and LDA analyses. See DOI: 10.1039/x0xx00000x

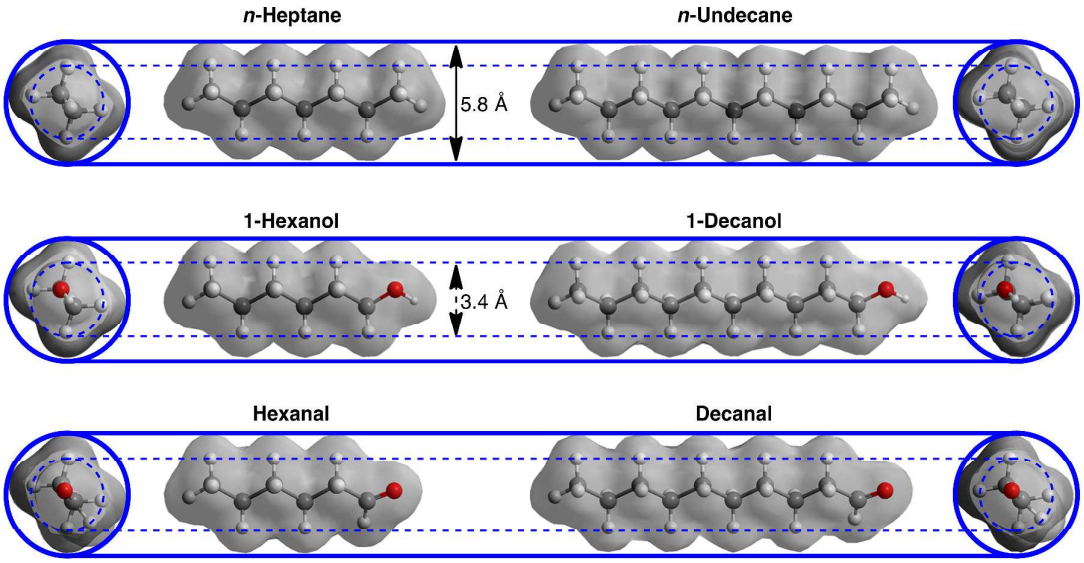

Fig. 1. Three-dimensional images of structural similarity of cluster numbers of 7 (left) and 11 (right). Carbon, hydrogen and oxygen atoms are shown in dark grey, light grey and red, respectively. The optimized structures of these compounds are simulated by MM2 using ChemBio3D Ultra (Cambridge Soft). Blue solid circles and lines, dashed circles and lines of diameters and width are same as 5.8 and 3.4 Å, respectively. van der Waals volume of each compound was listed in Table 1.

receptor materials, we focus on an inorganic nanoparticle with an organic functional group,[14–16] because of its high sensitivity stemming from the large Young's modulus of inorganic material as well as the tuneable selectivity by its organic functional groups. In this study, silica/titania-based hybrid nanoparticles with terminal amine functionality (NH_2-STNPs) were used as a receptor material of MSS. NH_2-STNPs were prepared through hydrolysis and co-condensation reaction with titanium tetraisopropoxide and aminopropyltriethoxysilane, combined with a multi-step microfluidic approach according to the previous report (details are described in Experimental Section).[14,15] NH_2-STNPs were coated on the surface of MSS by an spray coating (Fig. S1, ESI†).

We investigated the responses of NH_2-STNPs-coated MSS to the target molecules. According to the calculated van der Waals (vdW) volume by modified calculation method based on Bondi radii (Fig. S2, ESI†),[17,18] molecules with same number of cluster atoms (N_c) exhibit similar vdW volume (see also Table 1). We selected 6 odorous molecules as two series of the structurally similar molecules with the minimal physical effect on sensing signals as shown in Fig. 1: N_c = 7 (*n*-heptane, 1-hexanol, and hexanal) and N_c = 11 (*n*-undecane, 1-decanol, and decanal). We measured the gases from the sample liquids of these chemicals using the flow system controlled by mass flow controllers (MFCs) (Fig. S3, ESI†; Details are described in Experimental Section). From the physical point of view, same amount of molecules with similar molecular volume should obtain the similar intensity of a nanomechanical sensor,[8,11] while signal responses of the measured gases were different in terms of the intensity as well as the shape (Fig. 2; see also Fig. S4). These results can be attributed to the different chemical interactions with the terminal amines on the surface of STNPs, especially hydrogen bonding; alkanes, alcohols and aldehydes have different numbers of hydrogen bonding donor and acceptor sites (data is summarized in Table 1).

The MSS coated with NH_2-STNPs exhibited a concentration dependent signal response (Fig. 3; see also Fig. S5, ESI†) by changing P_a / P_o = 2, 5, 10%, where P_a and P_o indicate partial vapour pressure and saturated vapour pressure of samples, respectively. In general, for nanomechanical sensors including MSS, gas molecules adsorbed on a receptor layer induces surface stress, resulting in a response signal.[8] A certain amount of gas molecules are required to induce a measurable signal response. This trend is clearly observed in Fig. 3a and b; the decrease in the partial vapour pressure induces the delay in the starting point of a signal response as well as the suppression of maximum intensity. On the other hand, the signal of each vapour started decaying as soon as the desorption steps started irrespective of partial vapour pressure (Figs. 3c and 4). Although the sensing signal of nanomechanical sensors is determined by various phenomena including viscoelastic responses,[19] this behaviour could be basically attributed to the different baseline at the beginning of the desorption steps; the starting points of desorption were in the measurable range. It should be also noted that the MSS coated with NH_2-STNPs responded to gases with low concentrations, such as less than 100 ppb of 1-decanal;[12,‡] according to the signal (~1 mV/V) to noise (~1 μV/V) ratio, the limit of detection could reach down to 0.1 ppb level. In addition to the high sensitivity of MSS, this kind of behaviour is basically due to the intrinsic property of gas/solid equilibrium-based chemical sensors, for which the sensitivity depends not on the absolute concentration but on the partial vapour pressure.[20]

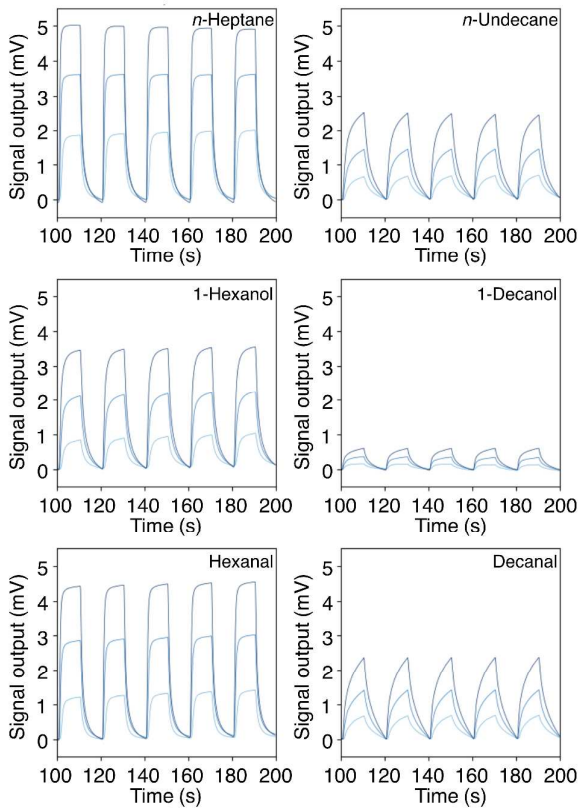

Fig. 2. The sensor responses to two series of structurally similar molecules: Series of N_c = 7 (Left) and 11 (Right). Lighter to darker colours indicate P_a / P_o of 2, 5 and 10%, respectively; where P_a and P_o stand for partial pressure and saturated vapour pressure of each sample, respectively. The latter 5 signals from 100 to 200 seconds out of 10 signals are shown. Full response signals are shown in Fig. S3, ESI†.

To identify the structurally similar molecules with different concentrations, appropriate features should be extracted from the sensing signals, especially the features related to the chemical information. The feature extraction methods have been widely studied for the pattern recognition, in which a large variety of features are reported.[21,22] While the signal intensity is basically determined by physical properties including structural similarity and partial vapour pressure, the adsorption and desorption slopes tend to reflect the chemical properties as can be seen in Figs. 3 and 4 (see also Fig. S5, ESI†). Thus, we extracted adsorption (m_{ai}) and desorption (m_{di}) slopes from each normalized signal response as features by following equations (1) and (2):

$$m_{ai} = \frac{I(t_i) - I(t_0)}{t_i - t_0}, \qquad I(t_0) = 0 \tag{1}$$

$$m_{di} = \frac{I(T_i) - I(T_0)}{T_i - T_0}, \qquad I(T_0) = 1 \tag{2}$$

where $I(t)$ indicates signal output at time t [s], and t_0 and T_0 correspond to the times when the signal starts to rise and decay, respectively (Fig. 5d and e). In this study, we set three time points as follows: $t_1 = t_0 + 0.5$, $t_2 = t_0 + 1.0$, $t_3 = t_0 + 1.5$, $T_1 = T_0 + 0.5$, $T_2 = T_0 + 1.0$ and $T_3 = T_0 + 1.5$ [s]. Six sets of the parameters ($m_{a1–3}$, $m_{d1–3}$) were extracted from the latter 5 signals from 100 to 200 seconds out of 10 signals in each response signal, since the latter cycles provide reproducible signals without initial fluctuations induced by mixing of sample gases and pre-adsorbed gases (see also Fig. S4, ESI†).

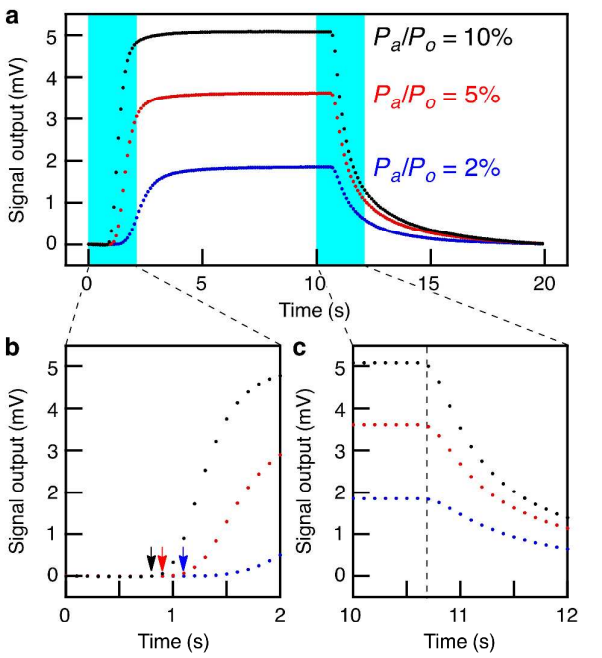

Fig. 3. Partial vapour pressure-dependent signal responses. (**a–c**) Overview and enlarged sensor responses of *n*-heptane with different P_a / P_o values. See also Figs. 5 and S4, ESI† for detailed signal responses.

To observe the overall contributions of the parameters, we first performed principal component analysis (PCA) on the dataset of all concentrations P_a / P_o (Fig. 5a) using all 6 features ($m_{a1–3}$, $m_{d1–3}$). Each molecule having N_c = 7 can be clearly distinguished from others with well-separated clusters in the principal component space. In the series of N_c = 11, on the other hand, 1-decanol can be distinguished from *n*-undecane and decanal, whereas *n*-undecane and decanal are overlapped (Fig. 5a; see also Fig. S6, ESI†). It is also found that each molecule was clearly divided into three different clusters corresponding to the different concentration. Thus, further feature selection is required to discriminate each molecule with less influence of the variation in concentration. Although a supervised analysis of linear discriminant analysis (LDA) can classify all 6 molecules with 96.7% accuracy including all concentrations P_a / P_o (Fig. S7, ESI†), an unsupervised PCA will provide another insight into an effective approach to more robust identification of chemical species by analysing the dataset without a label and maximizing the variance.

On the basis of the previous discussion on the differences of the signal responses during adsorption and desorption steps, we further investigated the relationship between the features and concentration. The use of only adsorption slopes ($m_{a1–3}$) as features for PCA resulted in densely overlapped clusters in the

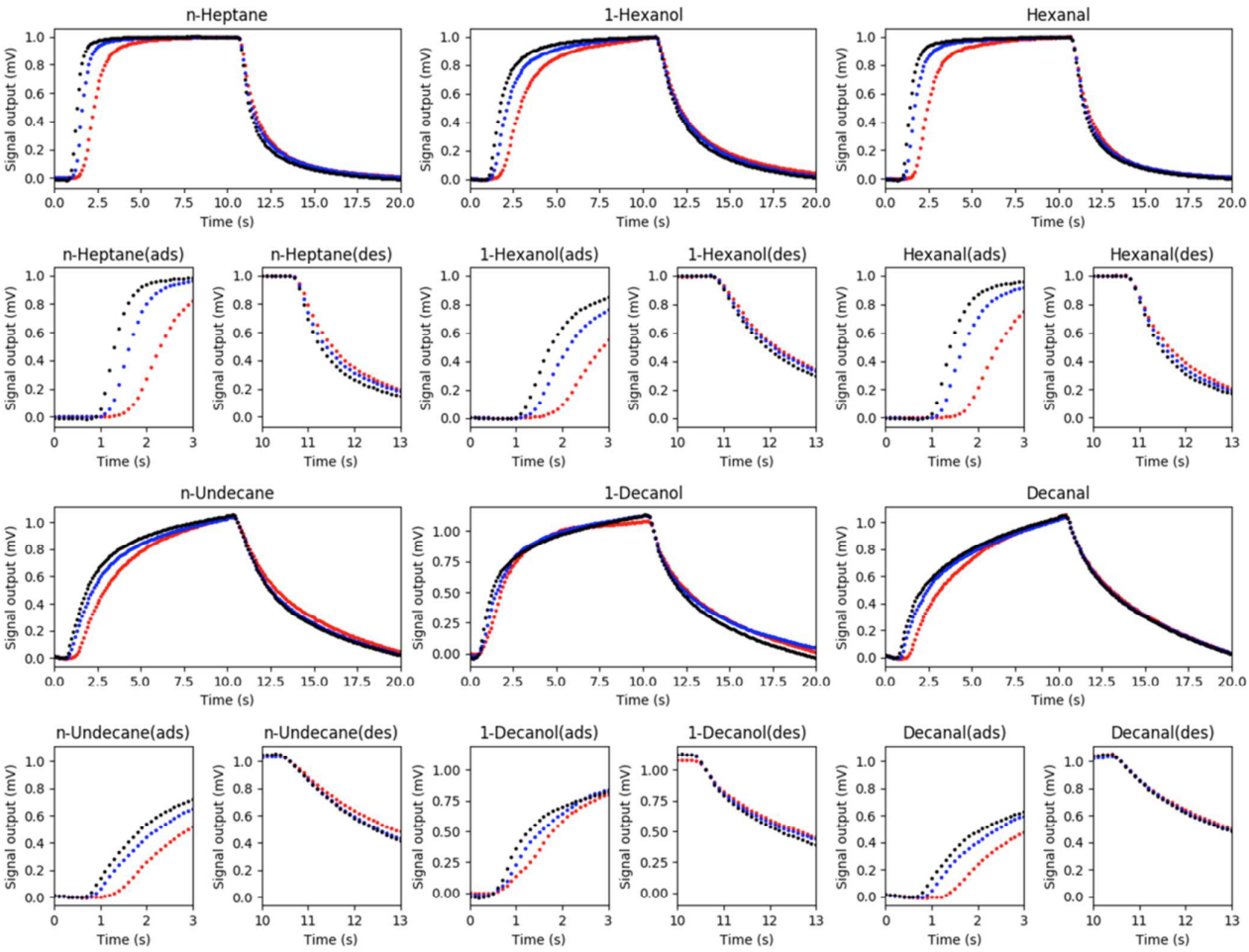

Fig. 4. Normalized signal responses of all chemicals measured in this study. One signal response cycle and enlarged signals at the starting time of adsorption (ads) and desorption (des).

principal component space as shown in Fig. 5b, suggesting that the adsorption slopes m_{a1-3} are strongly correlated to the concentration, reflecting the mechanism of the nanomechanical sensors discussed above. In contrast, when only desorption slopes (m_{a1-3}) were used for PCA, each molecule was well separated with a slight overlap (Fig. 5c). As demonstrated, the discrimination of odorous molecules in terms of chemical properties can be achieved by the features extracted from the desorption slopes, which have been found to be less affected by the variation in concentration.

Conclusions

We have demonstrated the discrimination of odorous molecules in a series of similar physical structures by the appropriate selection of signal features based on the mechanism of a nanomechanical sensor. Such robust identification of chemical species will enhance the potential of nanomechanical sensors for various applications. Recently, we also reported quantitative prediction of specific information in complex odours using machine learning, in which careful screening of extracted features played a vital role. Thus, it is important to select effective features from sensing signals depending on each purpose. In the present study, the careful investigation of features based on the mechanism of nanomechanical sensors led to the finding of effective features in the desorption steps, which are less affected by the variation in concentrations. In other words, if concentration-dependent information is essential in some applications, one can utilize the features associated with the adsorption step. For some molecules which induce different olfactory sensation depending on the concentration, such concentration-dependent features will be effective. This study provides a guideline for effective feature extractions for both concentration-dependent/-independent applications through nanomechanical sensors. Another important aspect of this study is the feasibility demonstration of the detection and discrimination of odorous molecules, which can be found in human body odours.[23,24] Since the body odours are known as indicators of various health conditions, nanomechanical sensors will be also able to contribute to such applications.

Experimental Section

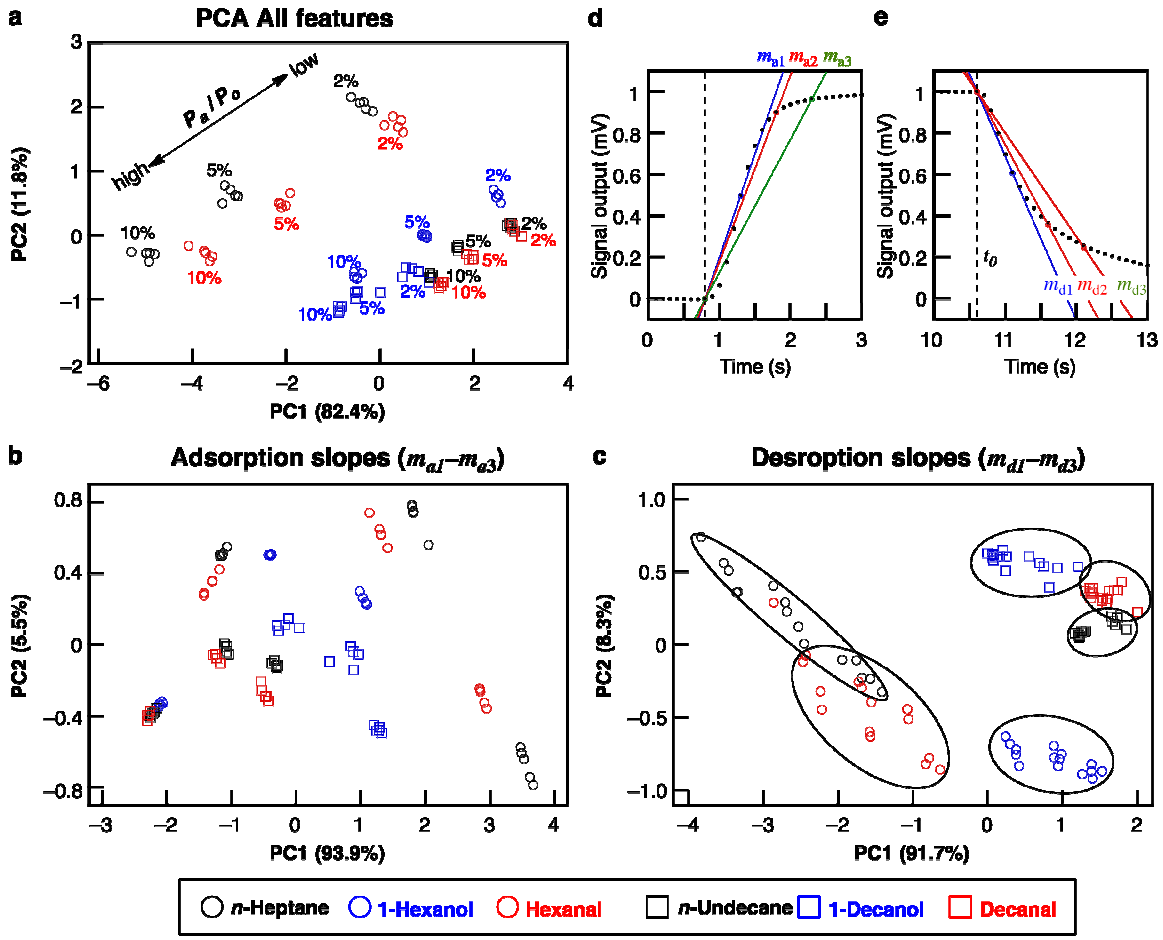

Fig. 5. (**a**) Principal Component Analysis (PCA) score plots for the structurally similar molecules. All six features from adsorption and desorption slopes were used. Numbers in % indicate partial vapour pressure P_o / P_o of the corresponding plots. (**b, c**) PCA score plots obtained by the features from only adsorption slopes (**b**) and those from only desorption slopes (**c**). Circle and square correspond to the number of cluster atoms of 7 and 11, respectively. Black, blue and red colours indicate alkane, primary alcohol and aldehyde, respectively. (**d**, **e**) Feature extraction methods from (**d**) adsorption (m_{a1}, m_{a2}, m_{a3}) and (**e**) desorption (m_{d1}, m_{d2}, m_{d3}) curves.

Materials

Aminopropyltetraethoxysilane (APTES; Sigma-Aldrich Inc.), titanium tetraisopropoxide (TTIP; Tokyo Chemical Industry Co., Ltd.) and isopropyl alcohol (IPA; Wako Pure Chemical Industries, Ltd.) were purchased, and used as received. *n*-Heptane, 1-hexanol, hexanal, *n*-undecane, 1-decanol and decanal were purchased from Sigma-Aldrich, Tokyo Chemical Industry, Wako Pure Chemical Industries and used as received.

Preparation of NH_2-STNPs

Silica/titania-based hybrid nanoparticles functionalized with aminopropyl groups (NH_2-STNPs) were prepared by a multi-step nucleation controlled growth method reported previously.[15] Briefly, 5 starting solutions (Solutions A–E) were prepared. The Solutions A (APTES, 1.48 mL; IPA, 8.64 g), B (28%-NH_3 aq., 0.758 g; ultrapure water, 2.84 g; IPA, 6.98 g), C (TTIP, 0.458 mL; IPA, 9.44 g), and D (ultrapure water, 0.078 g; IPA, 9.74 g) were individually flowed in perfluoroalkoxyalkane (PFA, 1.0 mm inner diameter, 1/16 inch outer diameter, product of YMC Co., Ltd.) tubes with a syringe pump (CXN1070, product of ISIS, Co., Ltd.) at 10 mL/min. The solutions A and B, and Solutions C and D were mixed respectively in a polytetrafluoroethylene (PTFE) fluidic channel with a Y shape junction (the channel cross section of approx. 1 mm^2, KeyChem mixer, product of YMC Co., Ltd.). After that, resultant 2 reaction solutions, *i.e.* Solution A + B and Solution C + D, were mixed in the second fluidic channel placed just after the first two fluidic channels. The first and second fluidic channels were connected with 10 cm PFA tubes. Then, the mixture of the 4 Solutions A–D was flowed through a PFA tube with 70 cm in length and was added into the Solution E (ODA, 0.137 g; ultrapure water, 40 g, IPA: 123 g) under magnetic stirring. After the addition, the final reaction solution was aged at room temperature until it is used for coating.

Fabrication of MSS receptor layers

NH_2-STNPs was spray-coated onto the surface of MSS by using a spray coater (rCoater, product of Asahi Sunac Co.) after preparing a suspension. For the preparation of the NH_2-STNPs suspension, NH_2-STNPs were centrifuged at 9000 rpm for 20

min. The sediment was carefully washed with IPA several times and then IPA/water mixture (vol/vol = 3/5) was added. The concentration of the suspensions was set at approx. 1 g/L. Before spray-coating, the suspensions were fully ultrasonicated to get the NPs dispersed as much as possible (some aggregates were still recognized).

Then, the suspension was loaded in a syringe and was flowed through a PTFE tube at 3 mL/min by using a syringe pump (YSP-201, product of YMC Co., Ltd.). The suspension was introduced into a spray nozzle and then was sprayed with the help of two types of carrier air (atomizing air: 0.030 MPa, patterning air: 0.030 MPa) to form homogeneous droplets. An MSS chip was mounted on a stage which was heated at approx. 100 °C to quickly evaporate the droplets. The stage was moved back and forth, while the spray nozzle was also moved from left to right at 15 mm/s with 0.3 mm pitch. The distance between the spray nozzle and stage was set at 75 mm. The coating process was repeated to obtain coating thickness of a few micrometers.

Sensing system and procedure

The MSS chip coated with NH_2-STNPs was settled into a Teflon chamber and placed in an incubator with controlled temperature at 25.0 ± 0.5 °C (Incubator-1, Fig. S3, ESI†). The chamber was connected to a gas system consisting of two mass flow controllers (MFCs), a mixing chamber, a purging gas line and a vial for a target sample liquid in an incubator (Incubator-2) with controlled temperature at 15.0 ± 0.5 °C (Fig. S3, ESI†). The vapours of target samples were produced by bubbling of carrier gas. Pure nitrogen gas was used as carrier and purging gases. Total flow rate was kept at 100 mL/min during the experiments. The concentration of vapours were controlled by MFC-1 as P_a / P_o ranging from 2 to 10%; where P_a and P_o stand for the sample's partial vapour pressure and saturated vapour pressure, respectively.

Before measuring MSS signals, pure nitrogen gas was introduced into the MSS chamber for 1 min. Subsequently, the MFC-1 (sampling line) and MFC-2 (purging line) were switched every 10 [s] with controlled total flow rate at 100 mL/min through 10 cycles (Fig. 2; see also Fig. S4, ESI† for overall signal responses). Data were measured at the bridge voltage of –0.5 V, and recorded the relative resistance changes of piezoresistors with a sampling rate of 10 Hz. The data collection program was designed by LabVIEW (National Instruments Corporation).

Patternrecognition methods

Principal component analysis (PCA) and linear discriminant analysis (LDA) were used for discrimination of target samples. The PCA and LDA were used with '*R*' software ver. 3.3 and MASS package for the LDA. PCA finds projection weights for sensor response data that maximize the total response variance in principal components (PC), where the dimension capturing the greatest variance is given by PC1, and the second greatest variance (subject to being orthogonal to PC1) is given by PC2 the dimension capturing the second, and so on. LDA finds linear combinations of sensing features that separate tow or more classes of objects (samples). The classification accuracy was calculated by leave-one out cross validation using '*R*' software. The features used for the pattern recogntition were extracted as followed eqs. (1) and (2) from each normalized signal response.

Conflicts of interest

There are no conflicts to declare.

Table 1. Physical properties and chemical structures of series-7 and -11.

Chemicals	Chemical structure	N_c[a]	Sat. vapour pressure[b] [mmHg]		Biling Point [°C]	vdW volume[c] [Å^3]	# H-bonding sites	
							Donors	Acceptors
n-heptane		7	26.7		98	129.66	0	0
1-hexanol		7	<10.0	(0.55)[d]	157	121.15	1	1
hexanal	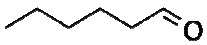	7	<10.0	(5.7)[e]	129	118.51	0	1
n-undecane		11	<10.0	(0.12)[f]	196	198.86	0	0
1-decanol		11	<10.0	(0.0037)[g]	230	190.35	1	1
decanal		11	<10.0	(0.029)[h]	207	187.71	0	1

[a] Number of cluster atoms, which indicate number of all atoms excluded hydrogen atoms. [b] Saturated vapour pressures at 15 °C were estimated by Antoine equation (Ref. 12). Most of chemicals excluding *n*-heptane are out of temperature range of the Antoine equation, because of the high boiling points of chemicals. Thus, values represents in this table are estimated with lowest temperature, and the saturated vapour pressures at 15 °C are shown in parentheses. [c] Calculated by the equation in Refs. 17 and 18. See also ESI†. [d–h] The lowest temperatures of *d–h* used for calculation are 55.08, 24.08, 75,17, 117.11 and 95.07 °C, respectively.

Acknowledgements

We thank Ms. Takako Sugiyama (WPI-MANA, NIMS) for the nanoparticle synthesis, and Ms. Yuko Kameyama, Ms. Keiko Koda and Ms. Eri Sakon (WPI-MANA, NIMS) for the coating of the receptor layers and data collection. This work was supported by the MSS alliance; JST CREST (JPMJCR1665); Grant-in-Aid for Scientific Research (A), 18H04168, MEXT, Japan; Center for Functional Sensor & Actuator (CFSN), NIMS; World Premier International Research Center Initiative (WPI) on Materials Nanoarchitectonics (MANA), NIMS.

Notes

‡ Saturated vapour pressures at 15 °C were estimated by Antoine equation (Ref. 12). Most of chemicals excluding *n*-heptane are out of temperature range of the Antoine equation, because of the high boiling points of chemicals. Thus, values represents in this table are estimated with lowest temperature, and the saturated vapour pressures at 15 °C are shown in parentheses in Table 1.

References

1 M. Brattoli, E. Cisternino, P. R. Dambruoso, G. de Gennaro, P. Giungato, A. Mazzone, J. Palmisani and M. Tutino, *Sensors*, 2013, **13**, 16759–16800.
2 G. Konvalina and H. Haick, *Acc. Chem. Res.*, 2013, **47**, 66–76.
3 J. Gutiérrez and M. C. Horrillo, *Talanta*, 2014, **124**, 95–105.
4 R. A. Potyrailo, *Chem. Rev.,* 2016, **116**, 11877–11923.
5 J.-W. Yoon and J.-H. Lee, *Lab Chip*, 2017, **17**, 3537–3557.
6 S. K. Jha and K. Hayashi, *Sens. Actuators B. Chem.*, 2015, **206**, 471–487.
7 B. Wang, T.-P. Huynh, W. Wu, N. Hayek, T. T. Do, J. C. Cancilla, J. S. Torrecilla, M. M. Nahid, J M. Colwell, O. M. Gazit, S. R. Puniredd, C. R. McNeill, P. Sonar and H. Haick, *Adv. Mater.*, 2016, **28**, 4012–4018.
8 G. Yoshikawa, T. Akiyama, S. Gautsch, P. Vettiger and H. Rohrer, *Nano Lett.*, 2011, **11**, 1044–1048.
9 G. Yoshikawa, T. Akiyama, F. Loizeau, K. Shiba, S. Gautsch, T. Nakayama, P. Vettiger, N. F. de Rooij and M. Aono, *Sensors*, 2012, **12**, 15873–15887.
10 G. Imamura, K. Shiba and G. Yoshikawa, *Jpn. J. Appl. Phys.*, 2016, **55**, 1102B3.
11 J. K. Gimzewski, C. Gerber, E. Meyer and R. R. Schlittler, *Chem. Phys. Lett.*, 1994, **217**, 589–594.
12 C. C. Yaws, *The Yaws Handbook of Vapor Pressure, Antoine Coefficients*, 2nd Edition, (Springer, New York), 2015.
13 G. Yoshikawa, *Appl. Phys. Lett.*, 2011, **98**, 173502.
14 K. Shiba, R. Tamura, G. Imamura and G. Yoshikawa, *Sci. Rep.*, 2017, **7**, 3661.
15 K. Shiba, T. Sugiyama, T. Takei and G. Yoshikawa, *Chem. Commun.*, 2015, **51**, 15854–15857.
16 I. Osica, G. Imamura, K. Shiba, Q. Ji, L. K. Shrestha, J. P. Hill, K. J. Kurzydłowski, G. Yoshikawa and K. Ariga, *ACS Appl. Mater. Interfaces*, 2017, **9**, 9945−9954
17 A. Bondi, *J. Phys. Chem.*, 1964, **68**, 441–451.
18 Y. H. Zhao, M. H. Abraham and A. M. Zissimos, *J. Org. Chem.* 2003, **68**, 7368–7373.
19 S. M. Heinrich, M. J. Wenzel, F. Josse and I. Dufour, *J. Appl. Phys.*, 2009, **105**, 124903.
20 B. J. Doleman, E. J. Severin and N. S. Lewis, *Proc. Natl. Acad. Sci. U. S. A.*, 1998, **95**, 5442–5447.
21 J. Yan, X. Guo, S, Duan, P. Jia, L. Wang, C. Peng and S. Zhang, *Sensors*, 2015, **15**, 27804–27831.
22 S. M. Scott, D. James and Z. Ali, *Microchim. Acta*, 2007, **156**, 183–207.
23 B. de Lacy Costello, A. Amann, H. Al-Kateb, C. Flynn, W. Filipiak, T. Khalid, D. Osborne and N. M. Ratcliffe, *J. Breath Res.*, 2014, **8**, 014001.
24 S. Haze, Y. Gozu, S. Nakamura, Y. Kohno, K. Sawano, H. Ohta and K. Yamazaki, *J. Investigative Dermatology*, 2001, **116**, 520–524.

Graphical Abstract

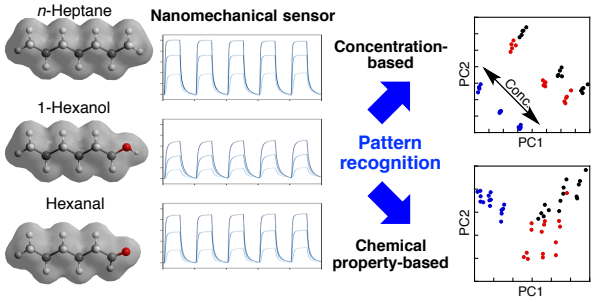

Structurally similar odours can be discriminated based on the chemical properties with reduced influence of their concentrations in a wide range from ppm to ppb levels by a pattern recognition using a nanomechanical sensor.